Supplemental Information

A New Murine Esophageal Organoid Culture Method and Organoid-Based Model of Esophageal Squamous Cell Neoplasia

Supplemental Figures

Figure S1

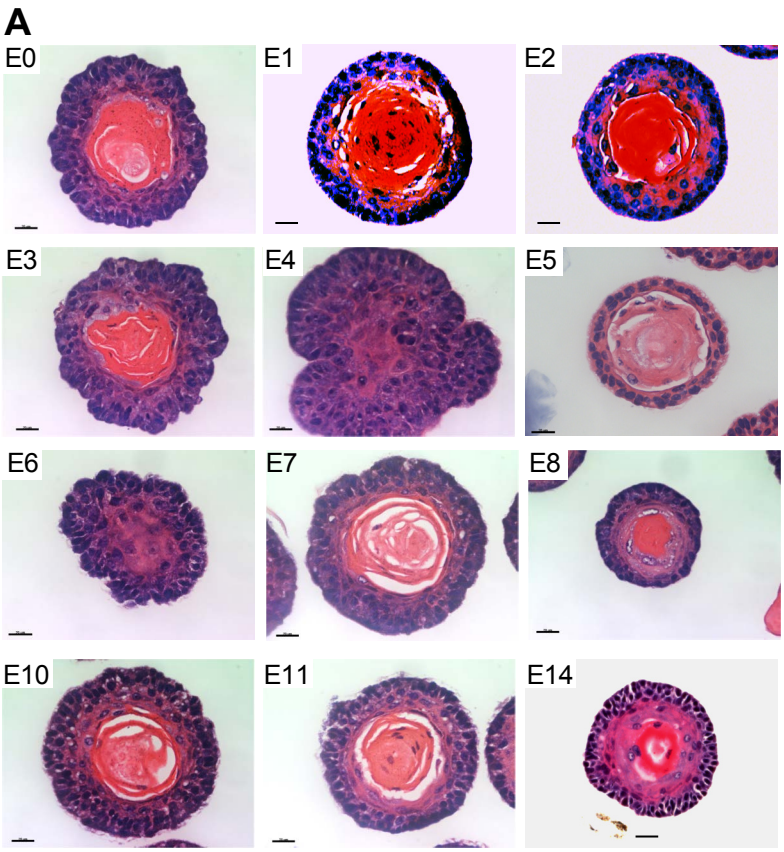

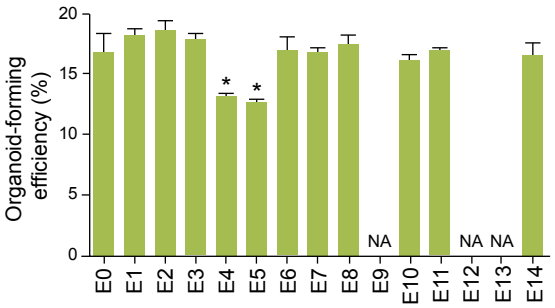

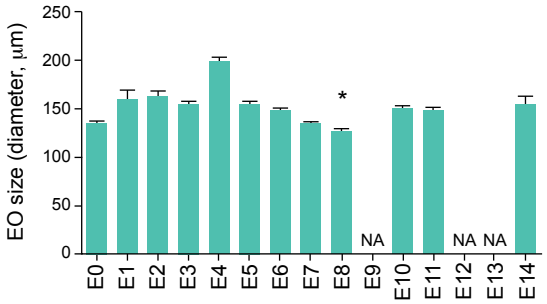

D

	E0	E14	WRN	W	R	N	RN	WN	WR
50% WRN medium [b]	+	+	-	-	-	-	-	-	-
Wnt	-	-	+	+	-	-	-	+	+
R-Spondin	-	-	+	-	+	-	+	-	+
Noggin	-	-	+	-	-	+	+	+	-

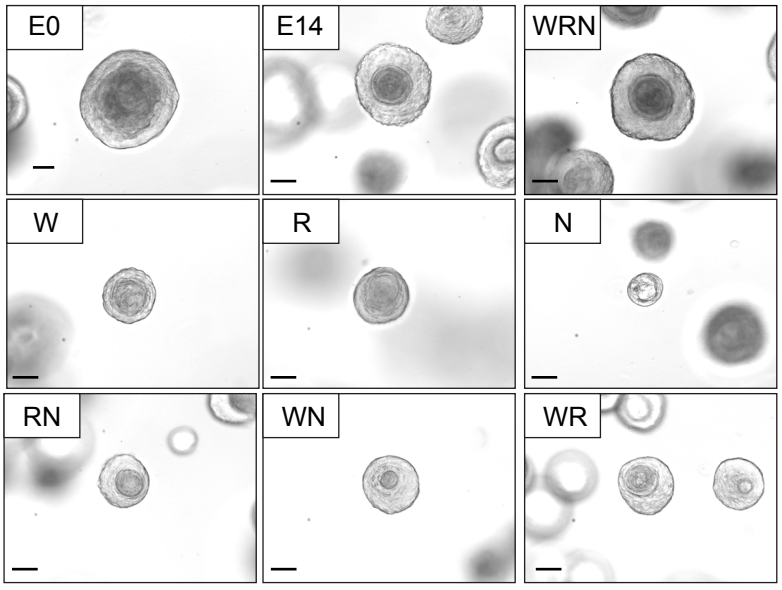

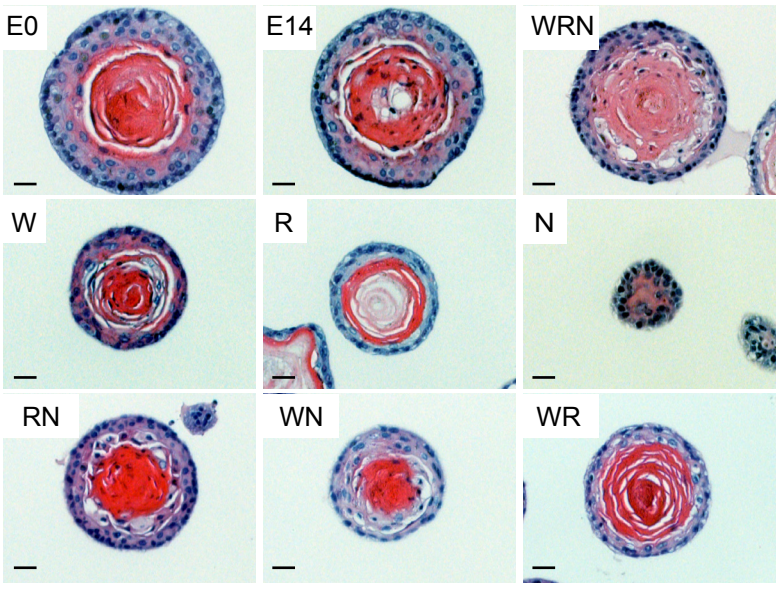

Figure S1. Comparative analysis of esophageal culture media, Related to Figure 1.
(A) Histologic analysis of EOs. The morphology of EOs was analyzed by H&E staining at d7 in different esophageal culture media. Scale bars, 20 μm.
(B-C) Quantification of the forming efficiency (B) and the size of EOs (C) in different esophageal culture media.
(D) Components of WRN-conditioned medium were tested to compare organoid forming efficiency. E0 and E14 media were used as controls and the other media were prepared based on E14 medium without 50 % WRN medium. WRN: Wnt, R-Spondin, Noggin recombinant proteins included, W: Wnt recombinant protein included, R: R-Spondin recombinant protein included, N: Noggin included, RN: R-Spondin and Noggin recombinant proteins included, WN: Wnt and Noggin recombinant proteins included, WR: Wnt and R-Spondin recombinant proteins included.
(E-F) Bright-field images and H&E staining images of organoids grown in different culture media. Scale bars, 20 μm.

Images are representative of three experiments with similar results. NA, not available. Error bars indicate mean ± s.d. *, $P<0.05$; groups were compared via one-way analysis of variance (ANOVA).

Figure S2

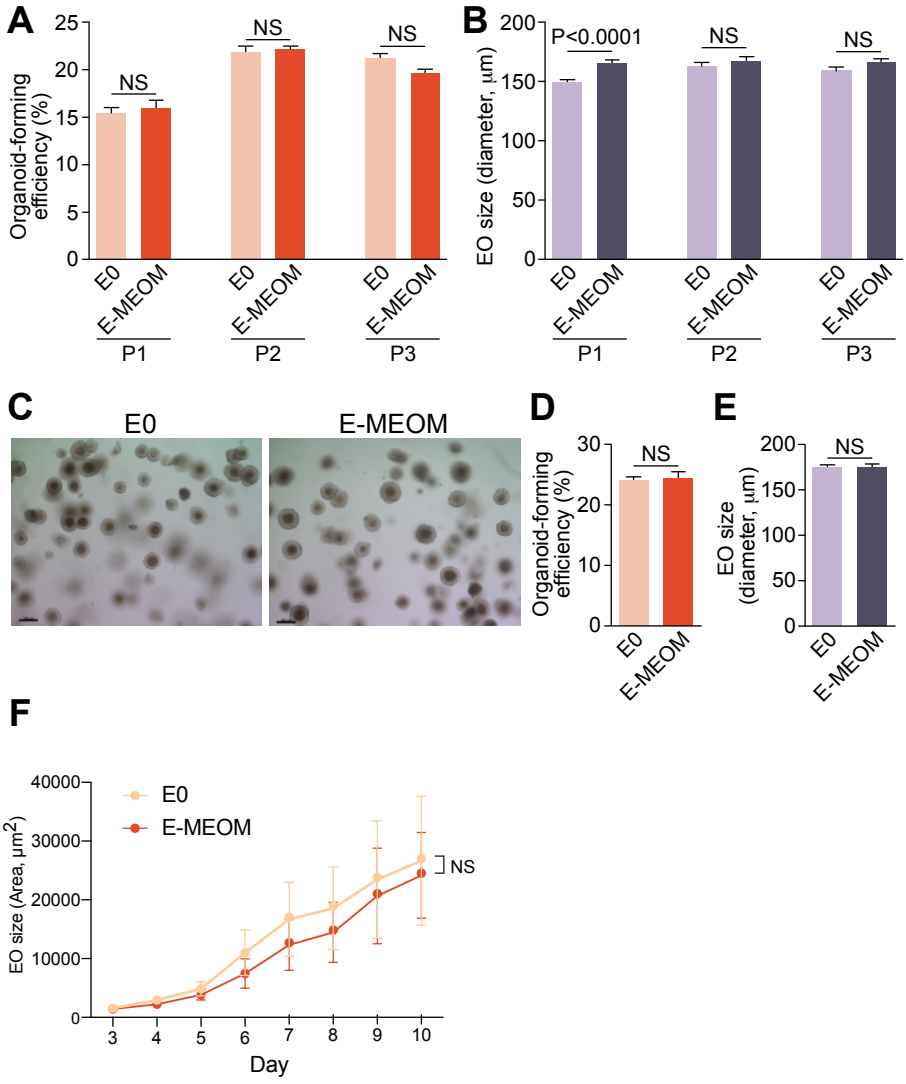
A
Organoid-forming efficiency (%)
25
20
15
10
5
0
NS
NS
NS
E0
E-MEOM
P1
P2
P3
B
EO size (diameter, μm)
200
150
100
50
0
P<0.0001
NS
NS
C
E0
E-MEOM
D
Organoid-forming efficiency (%)
30
20
10
0
NS
E
EO size (diameter, μm)
200
150
100
50
0
NS
F
EO size (Area, μm2)
40000
30000
20000
10000
0
E0
E-MEOM
NS
3
4
5
6
7
8
9
10
Day

Figure S2. Passage analysis of EOs cultured in E-MEOM, Related to Figure 2.
(A, B) Passage analysis of EOs cultured in E0 and E-MEOM. Equivalent growth of EOs was observed in E0 and E-MEOM during passages. (A) Organoid-forming efficiency. (B) Size.
(C-E) Growth of EOs in E-MEOM after freezing-thawing of EO single-cell suspension. EOs were observed in E0 and E-MEOM during the freezing-thawing process. (C) Bright-field images of EOs grown in E0 and E-MEOM (d7 after thawing). Scale bars, 200 μm. (D) Organoid-forming efficiency. (E) Size.
(F) Growth kinetics of organoids cultured in E0 and E-MEOM were plotted as a line graph. Images are representative of three experiments with similar results. Error bars indicate mean ± s.d. NS, not significant. Groups were compared via a two-sided unpaired *t*-test.

Figure S3

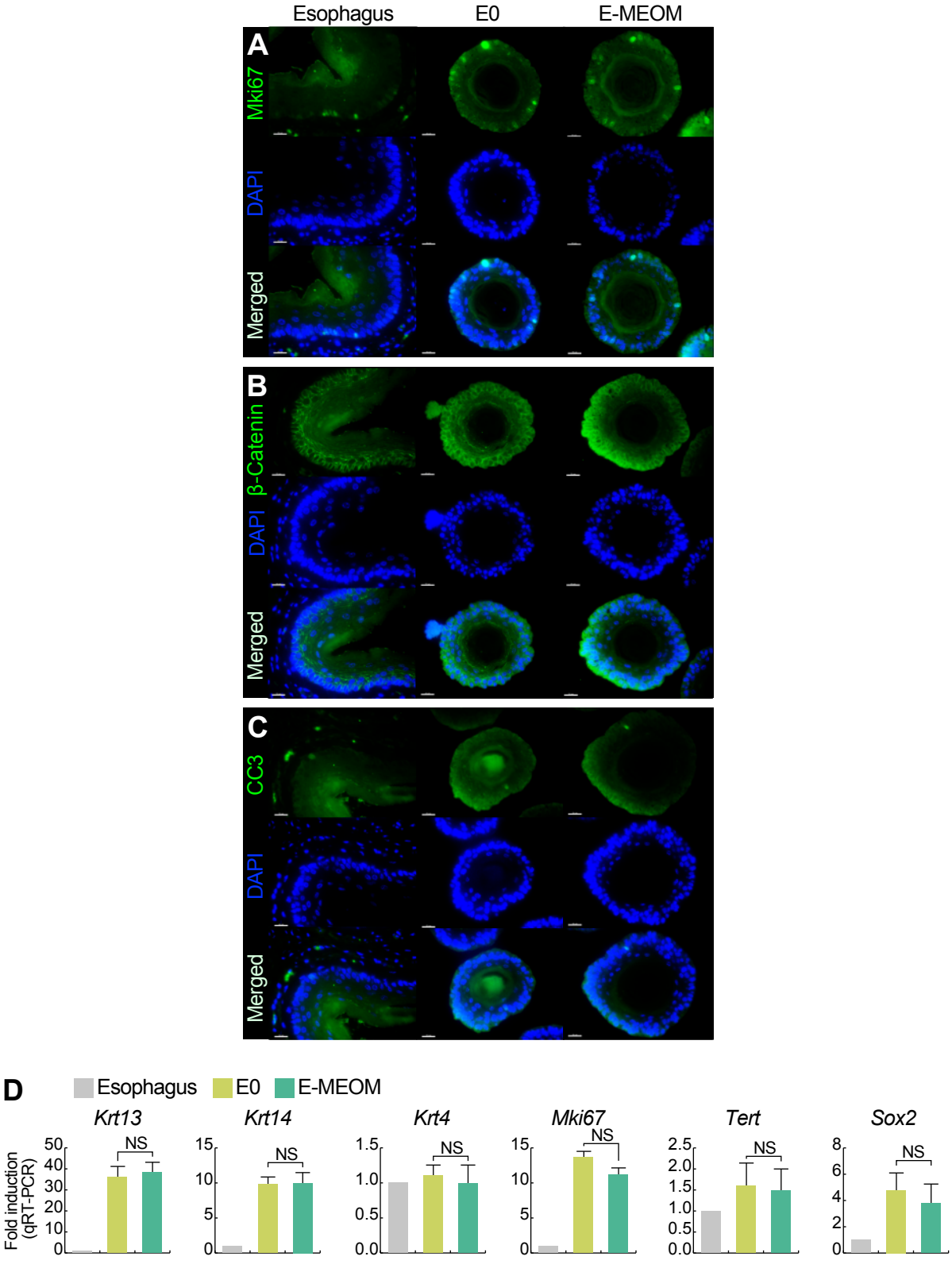
Esophagus
E0
E-MEOM
A
Mki67
DAPI
Merged
B
β-Catenin
DAPI
Merged
C
CC3
DAPI
Merged
D
Esophagus
E0
E-MEOM
Krt13
Krt14
Krt4
Mki67
Tert
Sox2
Fold induction (qRT-PCR)
NS

Figure S3. Expression of esophageal epithelium markers in the esophagus and in EOs cultured in E-MEOM and E0 medium, Related to Figure 3**.**

(A-C) Immunofluorescent staining of Ki67 (A), β-catenin (B), and cleaved caspase-3 (CC3) (C). Similar staining patterns were observed between EOs cultured in E0 and E-MEOM medium

(D) qRT-PCR for mRNA analysis of *Ck13*, *Ck14*, *Ck4*, *Mki67*, *Tert*, and *Sox2*. Similar gene expression patterns were observed between EOs cultured in E0 and E-MEOM medium.

Scale bars, 20 μm.

All images are representative of three experiments. Error bars indicate mean ± s.d. Groups were compared via one-way ANOVA.

Figure S4

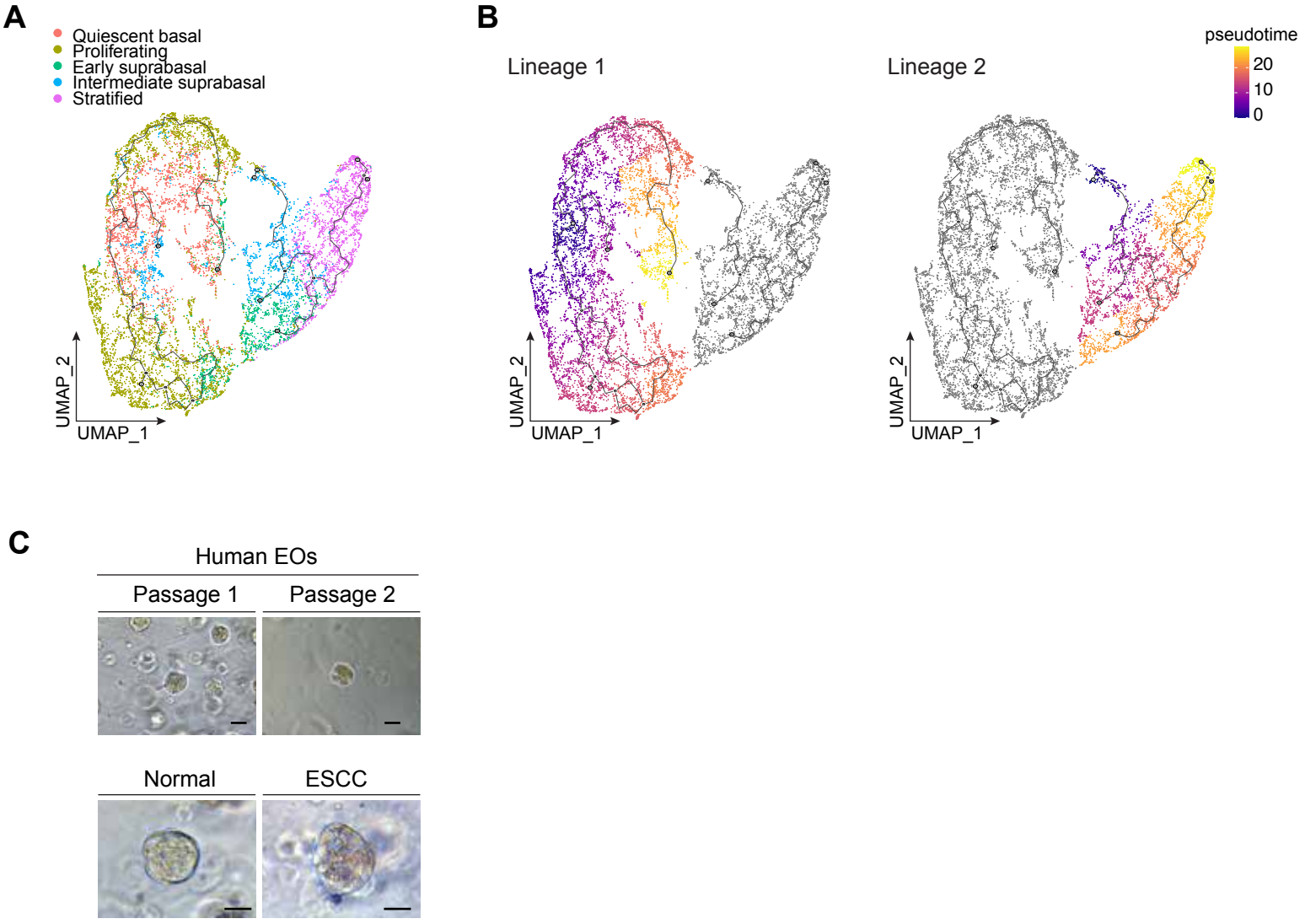
A
Quiescent basal
Proliferating
Early suprabasal
Intermediate suprabasal
Stratified
UMAP_2
UMAP_1
B
Lineage 1
Lineage 2
pseudotime
20
10
0
UMAP_2
UMAP_1
UMAP_2
UMAP_1
C
Human EOs
Passage 1
Passage 2
Normal
ESCC

Figure S4. Trajectory inference of mouse EO cells and human EO grown in E-MEOM, Related to Figure 4**.**

(A) Differentiation trajectory of mouse EO cells. The cell types are marked with different colors. Edges and connected lines in the graph show the trajectory defined by Monocle 3.

(B) Two lineages of each subtrajectory from (A) were visualized and colored by pseudotime. The lines were developed and learned by Monocle 3, which shows the graphical paths of differentiation.

(C) human esophageal cells were isolated from ESCC patients with cancer tissues and adjacent normal tissues and organoids were grown with E-MEOM medium for 10 days from single cells. Organoids with different passages (passage 1 and passage 2) were monitored, and the representative images of normal tissue-derived organoids were shown. Bright-field images of normal tissue- and ESCC-derived human esophageal organoids images were taken.

Scale bars, upper panels 50 μm, bottom panels 20 μm.

Figure S5

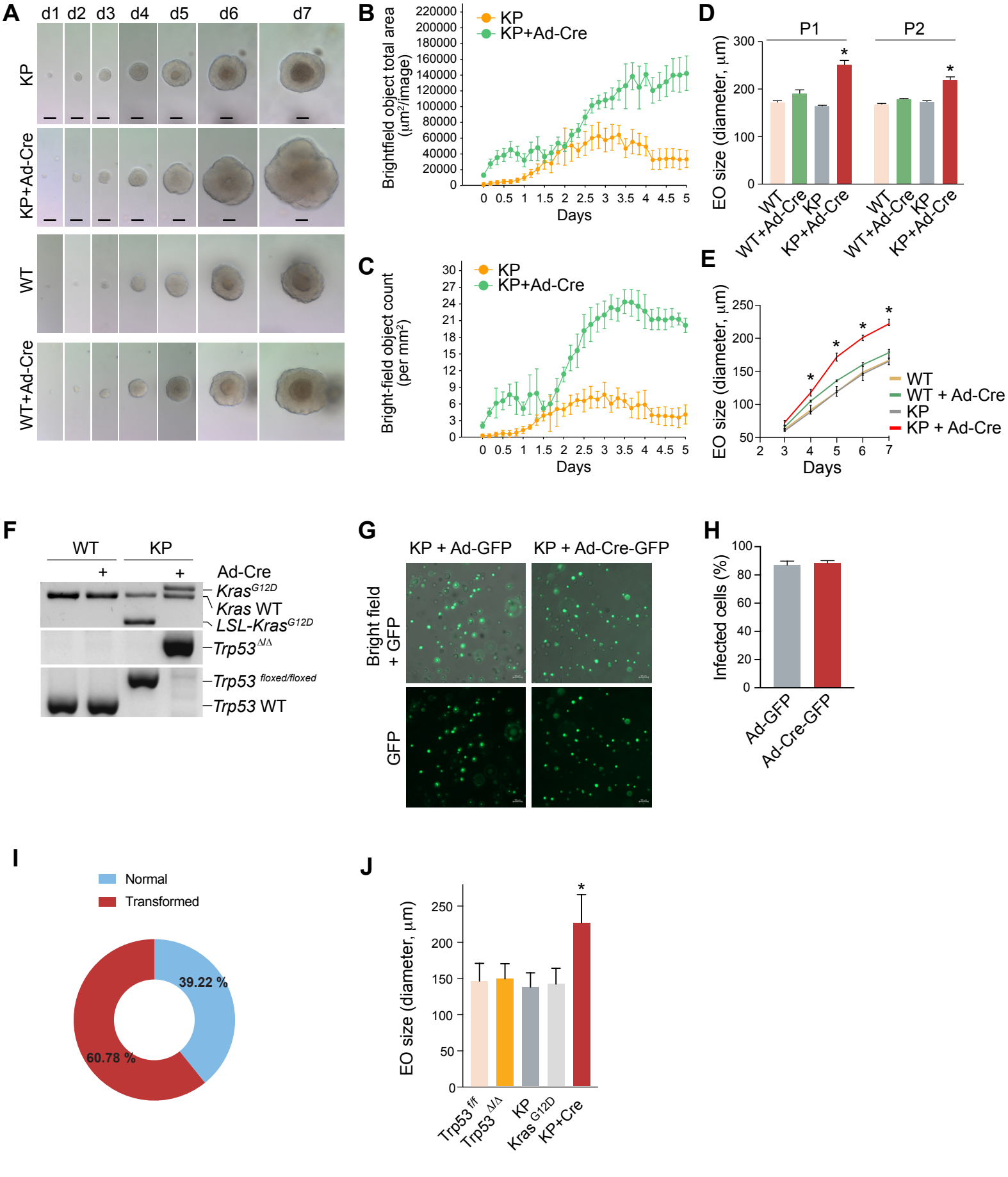
A
d1 d2 d3 d4 d5 d6 d7
KP
KP+Ad-Cre
WT
WT+Ad-Cre
B
Brightfield object total area (μm²/image)
KP
KP+Ad-Cre
Days
C
Bright-field object count (per mm²)
KP
KP+Ad-Cre
Days
D
P1
P2
EO size (diameter, μm)
WT
WT+Ad-Cre
KP
KP+Ad-Cre
E
EO size (diameter, μm)
WT
WT + Ad-Cre
KP
KP + Ad-Cre
Days
F
WT
KP
+
+
Ad-Cre
Kras G12D
Kras WT
LSL-Kras G12D
Trp53 Δ/Δ
Trp53 floxed/floxed
Trp53 WT
G
KP + Ad-GFP
KP + Ad-Cre-GFP
Bright field + GFP
GFP
H
Infected cells (%)
Ad-GFP
Ad-Cre-GFP
I
Normal
Transformed
39.22 %
60.78 %
J
EO size (diameter, μm)
Trp53 f/f
Trp53 Δ/Δ
KP Kras G12D
KP+Cre

Figure S5. Neoplastic EOs by *Kras*^{G12D} and *Trp53* KO in E-MEOM, Related to Figure 5.

(A) Hyperproliferation of EOs in E-MEOM from cells with *Kras*^{G12D} and *Trp53* KO (KP and KP+Ad-Cre), and control organoids (WT and WT+Ad-Cre). Bright-field images (d1-d7) of *Kras*^{LSLG12D}*:Trp53*$^{floxed/floxed}$ (KP), *Kras*^{LSLG12D}*:Trp53*$^{floxed/floxed}$ + Ad-Cre (KP+Ad-Cre) EOs, WT and WT+Ad-Cre cultured in E-MEOM from single cells.

(B-C) Comparison of organoid growth and size between KP and KP+Ad-Cre. EOs' size (B) and number (C) were monitored and measured by time-lapse analysis using IncuCyte (n=6).

(D-E) Increased size of *KrasG12D*:*Trp53* KO EOs. Quantification of EO size in two different passages (D) and during 7 days of culture (E).

(F) Confirmation of genetic recombination in KP EOs after Ad-Cre induction. Deletion of Lox-Stop-Lox in front of *KrasG12D* oncogene and *Tp53* exon were confirmed by PCR-based genotyping of *Trp53* and *KrasG12D*.

(G-H) Evaluation of viral vectors infection efficiency of KP cells. KP EO cells were infected with Ad-GFP or Ad-Cre-GFP and seeded with Matrigel. Infected organoids were evaluated by GFP expression in fluorescence microscopy on day 3. Representative bright-field images and fluorescence images were shown (G), and the infected cell ratio was calculated by dividing the number of GFP positive organoids by the total number of organoids (Ad-GFP; n=378, Ad-Cre-GFP; n=345) (H).

(I) Proportion of transformed organoid of KP cells after Cre induction. Normal or transformed organoids were calculated by counting spheroid organoid and non-spheroid organoid in the microscopy, respectively. Non-spheroid organoids were identified only if they showed neoplastic morphology, such as loss of both polarity and centrally localized keratin pulp. Totally 102 organoids were counted at day 8 and plotted with a circle graph.

(J) Growth of 3 different genetic altered EOs (*Trp53*$^{\Delta/\Delta}$, *Kras*^{G12D}, and KP+Cre) and control (*Trp53*$^{f/f}$ and KP) EO were evaluated with their size. *Trp53*$^{f/f}$; n=149, *Trp53*$^{\Delta/\Delta}$; n=94, KP; n=84, *Kras*^{G12D}; n=117, KP+Cre; n=180.

Scale bars, 50 μm. All images are representative of three experiments. Error bars indicate mean ± s.d. *, P<0.05 compared to the other groups; one-way ANOVA.

Supplemental Tables

Table S1. Primers used for genotyping, Related to STAR Methods.

Gene	Name	Sequence (5' to 3')
Trp53	Trp53-F1	CACAAAAACAGGTTAAACCCA G
	Trp53-R1	AGCACATAGGAGGCAGAGAC
	Trp53-F2	CACAAAAACAGGTTAAACCCA G
	Trp53-R2	GAAGACAGAAAAGGGGAGGG
Kras^{LSLG12D}	Kras^{LSLG12D}-1	GTCTTTCCCCAGCACAGTGC
	Kras^{LSLG12D}-2	CTCTTGCCTACGCCACCAGCTC
	Kras^{LSLG12D}-3	AGCTAGCCACCATGGCTTGAGTAAGTCTGCA

Table S2. Primers used for qRT-PCR, Related to STAR Methods.

Gene	Name	Sequence (5' to 3')
Krt13	Krt13-F	AGCTGCAGTCCCAGCTCAGCAT
	Krt13-R	TGCTCCTCCACACTGCCGATCAT
Krt14	Krt14-F	AGGGAGAGGACGCCCACCTT
	Krt14-R	CCTTGGTGCGGATCTGGCGG
Krt4	Krt4-F	AGCTGGCCCAGATGCAGACACA
	Krt4-R	TGCGATGATGCCATCCAGGTCCA
Mki67	Mki67-F	AGAGCCTTAGCAATAGCAACG
	Mki67-R	GTCTCCCGCGATTCCTCTG
Tert	Tert-F	AGCGGGATGGGTTGCTTTTAC
	Tert-R	CACCCATACTCAGGAACGCC
Sox2	Sox2-F	GAGGGCTGGACTGCGAACT
	Sox2-R	TTTGCACCCCTCCCAATTC
Hes1	Hes1-F	GGTATTTCCCCAACACGCT
	hes1-R	GGCAGACATTCTGGAAATGA
Dll1	Dll1-F	TGAGCCAGTCTTTCCTTGAA

	Dll1-R	AGACCCGAAGTGCCTTTGTA